Journal of Power Sources 240 (2013) 60–65

Contents lists available at SciVerse ScienceDirect

Journal of Power Sources

journal homepage: www.elsevier.com/locate/jpowsour

Short communication

Enhanced-electrocatalytic activity of Pt nanoparticles supported on nitrogen-doped carbon for the oxygen reduction reaction

Shiming Zhang, Shengli Chen*

Hubei Key Lab. of Electrochemical Power Sources, Key Lab. of Analytical Chemistry for Biology and Medicine (Ministry of Education), Department of Chemistry, Wuhan University, Wuhan 430072, China

HIGHLIGHTS

- Catalyst of Pt nanoparticles supported on nitrogen-doped carbon black (Pt/NCB).
- Increased dispersion of Pt nanoparticles on the NCB in comparison of that on the pristine CB.
- Pt/NCB catalyst exhibits both higher surface area and higher area specific activity for the ORR.
- Spillover effect may be responsible for the enhanced activity.

ARTICLE INFO

Article history:
Received 22 December 2012
Received in revised form
26 March 2013
Accepted 26 March 2013
Available online 8 April 2013

Keywords:
Spillover
Nitrogen-doped carbon
Pt catalyst
Oxygen reduction reaction
Fuel cells

ABSTRACT

Spillover, a well-known phenomenon in heterogeneous catalysis referring to the transport of the adsorbed intermediates over the catalyst/support interface, could enhance the catalytic performance by providing additional active sites. Here, we report the spillover-promoted electrocatalytic activity of Pt supported on nitrogen-doped carbon black (NCB) for the oxygen reduction reaction (ORR). By treating Vulcan XC-72R carbon black (CB) at 600 °C under gaseous NH_3, NCB of near 1 at% surface nitrogen content is obtained. The catalyst of Pt supported on NCB (Pt/NCB) exhibits simultaneously smaller particle sizes and higher electrochemical surface area and electrocatalytic activity for the ORR than the catalyst of Pt supported on pristine CB (Pt/CB) prepared with the same impregnation method. Particularly, the activity enhancement of Pt/NCB over Pt/CB surpasses that expected due to the surface area increase, which seems to conflict with the common belief that Pt nanoparticles of smaller sizes would have lower area specific activities for the ORR. Cyclic voltammetric responses of these catalysts implied that the oxygenated adsorbates formed on Pt can transport to surface of the NCB support, which may be responsible for the increased area specific activity of the Pt/NCB catalyst.

1. Introduction

Proton exchange membrane fuel cells (PEMFCs) have attracted widespread attention due to their high energy density and low pollution [1,2]. Pt and/or its alloys are the state-of-the-art electrocatalysts for the oxygen reduction reaction (ORR) at the cathodes of PEMFCs. Due to the high cost and poor availability of Pt, one of the major efforts in current fuel cell research is to increase the utilization and durability of Pt-based electrocatalysts for the ORR so that the PEMFCs become commercially viable [3,4]. Usually, graphitized carbons of high surface areas are used as supports to increase the dispersion of Pt. However, the activities of the carbon-supported Pt catalysts of current states remain significantly below the requirement of the practical application of PEMFCs. In addition, Pt catalysts supported on carbon materials suffer from dissolution, aggregation and detaching during fuel cell operation [5,6].

Recently, a variety of nitrogen- (N) doped carbon materials, such as carbon nitride (CN_X) materials [7,8], mesoporous carbons [9], carbon nanofibers [10,11], carbon nanotubes [12,13], graphenes [14] and carbon black [15], have been evaluated as supports for enhancing the activity and durability of Pt catalysts for the ORR. The advantages of N-doped carbons as catalyst supports may include increasing the catalyst dispersion due to the developed pore structures [7–17], improving the electric conductivity [7–18], enhancing the adhesion of Pt nanoparticles due to charge transfer from Pt to the adjacent N atoms [7,8,12–17], helping to decompose the reactive intermediates such as hydrogen peroxide [8,12,14,16], and so on.

* Corresponding author.
E-mail address: slchen@whu.edu.cn (S. Chen).

0378-7753/$ – see front matter © 2013 Elsevier B.V. All rights reserved.
http://dx.doi.org/10.1016/j.jpowsour.2013.03.149

Spillover is another well-known catalyst-support coupling effect in heterogeneous catalysis and electrocatalysis, which refers to the transport of some intermediate adsorbates produced on the catalyst surface over the catalyst/support interface [19–21]. This effect could enhance the overall activity of a catalytic reaction if the spillover intermediates can further react on the support [19–21]. In this study, we show that the spillover effect may contribute to the ORR activity promotion of Pt supported on N-doped carbons by comparing the electrocatalytic properties of Pt nanoparticles supported on the Vulcan XC-72R carbon black heat-treated under gaseous argon and NH_3 respectively. The Vulcan carbon black is used since it is one of the commonly used support materials for the commercial Pt catalysts in fuel cells. In most of the previous studies, the N-doped carbon supports are based on various novel nanostructured carbon materials. The complex porous structures in these materials may bring about additional promoting/inhibiting effects in electrocatalytic performance.

Recent studies have shown that N-doping can increase the oxophilicity of the carbon materials, making the N-doped carbons themselves can be ORR active [22]. However, N-doped carbons mainly exhibited superior ORR activities in alkaline [23,24], and remain poorly active in acidic media [24,25]. This might be due to that these materials are not oxophilic enough to initiate the dissociation of O_2 at positive potentials where the ORR takes place in acid media. By comparing the cyclic voltammetric responses of Pt nanoparticles supported on the Ar-treated carbon black (denoted as ACB in the following) and NH_3-treated carbon black (denoted as NCB in the following), we speculate that the oxygenated adsorbates formed on Pt can transport to the active sites of the NCB support due to the increased oxophilicity of N-doping carbons. This makes the support participate in the ORR, therefore increases the apparent area specific activity of Pt. To the best of our knowledge, this should be among the first reports that the oxygen spillover as a catalyst-support synergetic effect can enhance the ORR activity of Pt supported on N-doped carbons.

2. Experimental

2.1. Preparation of catalysts

To prepare the NCB, certain amounts (300 mg) of Vulcan XC-72R carbon black (CB) was ultrasonically mixed with a small amount of $FeSO_4{\cdot}7H_2O$ (15 mg) in distilled water. After lyophilizing, the mixture was heat-treated at 600 °C in a tube furnace under the flowing NH_3 for 2 h. The obtained sample was soaked with 1 M H_2SO_4 to remove Fe, and then washed with distilled water. The NCB was finally obtained after drying overnight in a vacuum at 60 °C. As a reference support, ACB was prepared in the same procedure except that the heat-treatment was under the flowing argon. This can avoid the possible effect of the heating temperature on the support materials and makes that the two support materials differ from each other in the nitrogen-doping. In fact, such a heat-treatment of carbon blacks in Ar has been commonly used in preparing carbon-supported Pt catalysts, which can remove the adsorbed water and other impurities residing in the support.

Caron-supported Pt nanoparticle catalysts (Pt/NCB, Pt/ACB and Pt/CB) were prepared by the conventional impregnation method [26]. Briefly, the required amounts of chloroplatinic acid ($H_2PtCl_6{\cdot}6H_2O$) aqueous solution (0.077 mol L^{-1}, 0.83 mL) were mixed with the corresponding carbon support materials (NCB, ACB and CB) under ultrasonic stirring and heating till the solutions turning to slurry. After drying at 40 °C overnight and 80 °C for ca. 30 min, the resulted powders were heated in a tube furnace under flowing H_2 at 120 °C for 2 h. The total Pt loading was maintained at 20 wt% for all the prepared catalysts.

2.2. Physical characterizations

The crystalline structure of the support materials and the prepared catalysts was obtained by recording their X-ray powder diffraction (XRD) patterns on a D8 X-ray Diffractometer using Cu Kα radiation source operating at 40 kV and 40 mA. The XRD profiles are recorded at a scanning rate of 4° min^{-1} between 5° and 85°. The images of Transmission electron microscope (TEM) were characterized using a JEM-2010HT (Center for Electron Microscopy Wuhan University). X-ray photoelectron spectroscopy (XPS) measurements were performed using a Kratos Ltd. XSAM-800 spectrometer with a Mg Kα X-ray source, and the data were fitted using the software XPSPEAK41.

2.3. Electrochemical measurements

All the electrochemical measurements were carried out using a three-electrode cell in which the working electrode was the commonly used thin-film rotating disk electrode (RDE) made by coating the studying catalysts on a glass carbon substrate (GC, 5 mm diameter) with Nafion as binding agent. The loading of Pt was 30 μg cm^{-2} on GC. The reference electrode was a saturated calomel electrode (SCE) which was separated from the working electrode by a Luggin capillary. The counter electrode was a Pt foil. The supporting electrolyte was 0.1 M $HClO_4$ aqueous solution. All the potentials were expressed with the reversible hydrogen electrode (RHE) by calibrating the SCE reference electrode to the RHE scale. By measuring the steady-state polarization curves of the hydrogen electrode reactions on Pt/CB-loaded GC electrode in 0.1 M $HClO_4$ saturated with H_2, the RHE zero potential was estimated with the potential at which the current crossed zero.

3. Results and discussion

Fig. 1a shows the powder XRD patterns of the NCB and ACB carbon supports. They similarly exhibit the (002) diffraction peak of graphite at 2θ value of ca. 25° and the (100) diffraction peak at ca. 43.5°. Compared to the ACB, a slight shift of the (002) diffraction peak toward the negative 2θ value is seen for NCB, indicating that the N-doping leads to an increased interlayer spacing [27]. The XRD patterns of the prepared Pt/NCB and Pt/ACB catalysts are shown in Fig. 1b. In addition to the diffraction peaks associated with the supports, the catalyst samples give diffraction peaks at 2θ values of about 39.7°, 46.3°, 67.6°, and 81.5°, which correspond to the (111), (200), (220), and (311) diffractions in the face centered cubic (fcc) structured Pt. From the peak widths of the Pt (220) peaks, the average sizes of the Pt nanoparticles are estimated to be around 1.7 and 2.4 nm for Pt/NCB and Pt/ACB respectively according to the Scherrer's formula.

Fig. 2 shows the TEM images (left) and the Pt particle size distributions (right) for the Pt/NCB, Pt/ACB, and Pt/CB catalysts estimated with 200 particles. It can be seen that the catalyst particles in the Pt/NCB were homogeneously dispersed on the supports and had relatively narrow size distribution around 1.8 nm, while the Pt particle sizes in the Pt/ACB were around 2.3 nm and relatively more widely distributed in comparison of that in Pt/NCB. This is in consistency with previous reports which showed that the use of N-doped carbons as supports can lead to well-dispersed metal particles [7–17]. By comparing the TEM images in Fig. 2b and c, we can find that Pt/CB possessed the similar Pt particle sizes to that in Pt/ACB catalyst.

The X-ray photoelectron spectroscopy (XPS) analysis was used to the prepared Pt/NCB and Pt/ACB catalysts. Fig. 3a showed the XPS spectra of wide survey scan which confirmed the existence of Pt, C, O for the two materials and the content of N-doping for 0.8 at% in

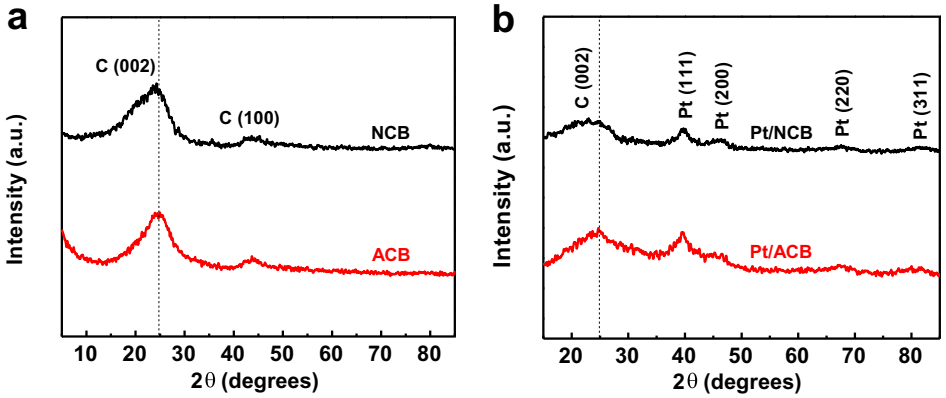

Fig. 1. XRD results of: (a) the different carbon support materials for NCB and ACB; and (b) the corresponding Pt-based catalysts for Pt/NCB and Pt/ACB.

Pt/NCB. As a reference, we could not find the peak of N in Pt/ACB. This seemed to prove that the transition metal serves to facilitate the stable incorporation of nitrogen into carbon matrix during the heat-treatment process [28,29]. By recording XPS spectra of N1s narrow-scans (Fig. 3b), we could deconvolved them into three different N functionalities which centered at 398.5 eV, 399.8 eV, and 401.1 eV, corresponding to pyridinic-N, pyrrolic-N, and graphitic-N respectively, predominantly in pyridinic form.

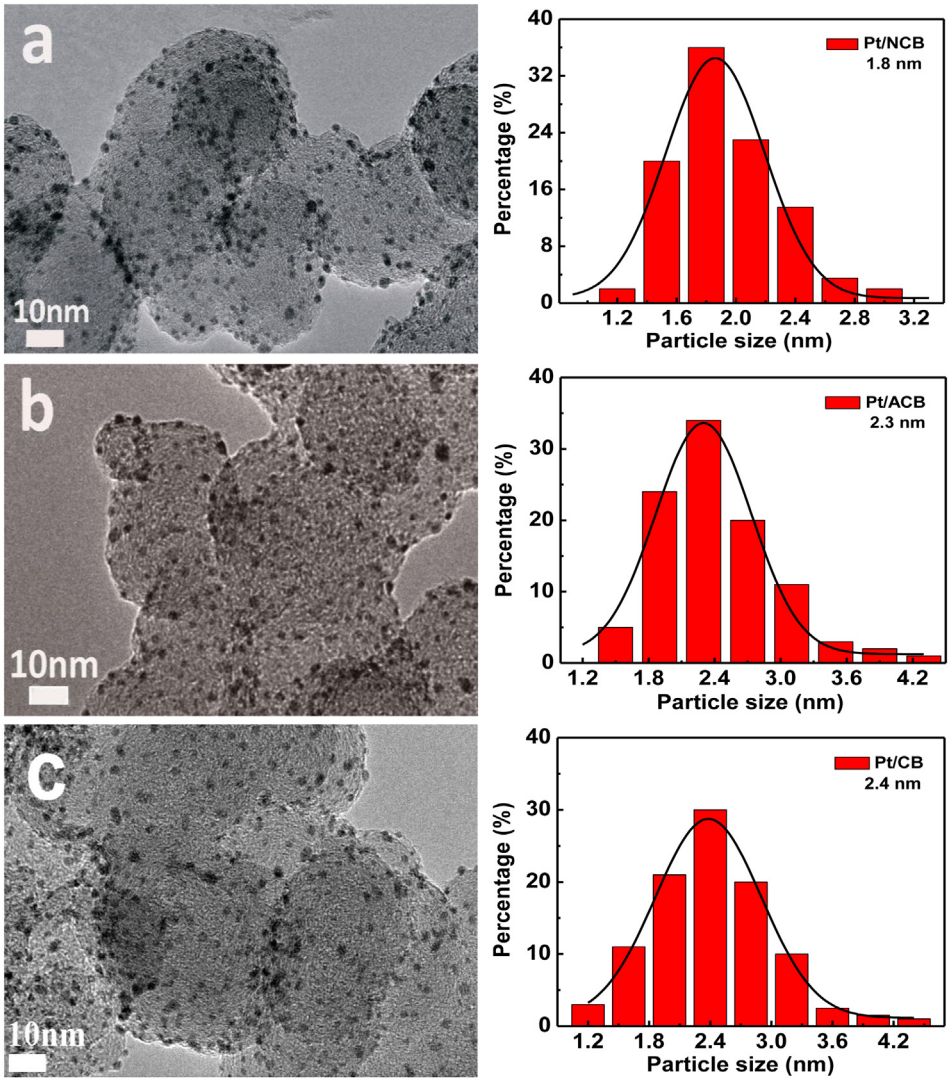

Fig. 2. TEM images (left) and particle size distributions (right) for (a) Pt/NCB, (b) Pt/ACB, and (c) Pt/CB.

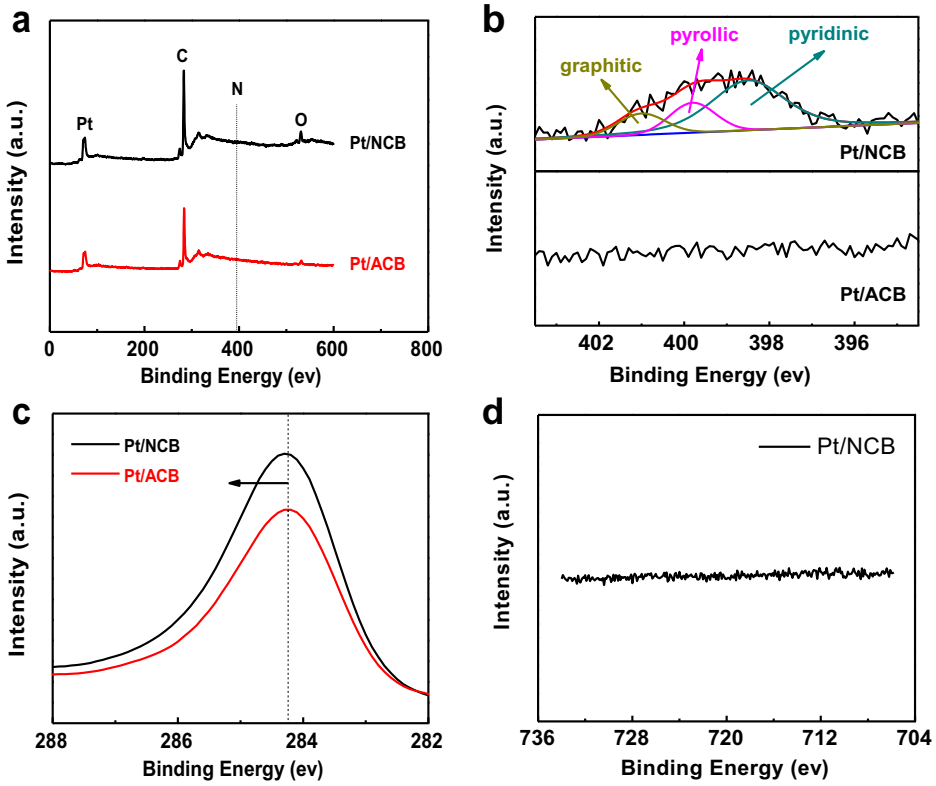

Fig. 3. XPS spectra of the prepared catalysts for Pt/NCB and Pt/ACB: (a) wide survey scan; (b) N1s narrow-scan and the corresponding deconvolution into components of different N functionalities and (c) C1s narrow-scan. (d) XPS spectra of Fe2p narrow-scan for Pt/NCB.

C1s spectrum of Pt/NCB had a more positive binding energy value compared to Pt/ACB in Fig. 3c. For Pt/NCB, the main peak position of C1s was 284.3 eV instead of 284.2 eV at Pt/ACB. This phenomenon had been found by Matter et al. [30] when heat-treating Vulcan XC-72 with acetonitrile (CH_3CN) at 900 °C. Also, Choi et al. [9] found it when carbonizing the resulting polypyrrole by chemical oxidation polymerization of the pyrrole monomers. It was expected that the positive shifted value of binding energy in C1s may due to the existence of C—N coordination. We also recorded the XPS spectrum of Fe2p narrow-scan (Fig. 3d) and the result suggested that Fe had been removed thoroughly from Pt/NCB.

Fig. 4a shows the typical ORR polarization curves of the prepared catalysts in O_2-saturated 0.1 M $HClO_4$ solutions at the room temperature. The Pt/NCB catalyst exhibited an ORR half-wave potential around 0.897 V, which is about 25 mV more positive than that given by the Pt/ACB catalyst. To better understand the difference in ORR activity, we calculated the mass and area specific activities of these catalysts for the ORR by normalizing the kinetic current at 0.9 V with the mass and the electrochemical surface area (ECSA) of the Pt on the GC electrode. The ECSAs, calculated by measuring the adsorption/desorption charges of the underpotential deposited hydrogen (Q_H) between 0 and 0.4 V on the cyclic voltammetric (CV) curves recorded for the catalysts in Ar-purged 0.1 M $HClO_4$ solution (Fig. 4b) after double-layer correction and assuming a value of 210 mC cm^{-2} for the adsorption of a hydrogen monolayer [31], were estimated to be 168.2 and 133.0 m^2 (g Pt)$^{-1}$ for Pt/NCB and Pt/ACB respectively. The higher ECSA of the Pt/NCB is due to the relatively smaller Pt particles as displayed in the TEM image (see Fig. 2a). As seen in Fig. 4c, the Pt/NCB catalyst exhibits a mass activity of ca. 0.180 A (mg Pt)$^{-1}$, which is about 2.1 times greater than that of Pt/ACB (0.087 A (mg Pt)$^{-1}$). The area specific activities of the two catalysts were found to be 0.107 mA cm^{-2} and 0.065 mA cm^{-2} respectively for Pt/NCB and Pt/ACB (Fig. 4d). As seen in the insets of Fig. 4a and b, Pt/CB exhibited very similar ORR polarization curve and CV to Pt/ACB. The ECSA was estimated to be ca. 122.8 m^2 (g Pt)$^{-1}$ for Pt/CB. Accordingly, Pt/CB exhibits very close mass and area activities for the ORR to Pt/ACB (Fig. 4c and d). It is worth mentioning that these measurements were carried out more than three times and the results showed good reproducibility.

It is now generally known that the area specific activity of nanoparticulate Pt catalysts for the ORR decreases with the Pt particle size [32–35]. Kinoshita [32] has summarized the results of the Pt particle size effect on the ORR kinetics from different studies and concluded that the area specific activity for the ORR decreased with decreasing the Pt particle size so that the mass activity exhibits a maximum around 3–3.5 nm. This particle size effect has been explained in terms of the increased fraction of edge atoms on Pt nanoparticle surfaces with the decreased particle size [32,35]. One thus should expect that Pt/NCB has lower mass and area specific activities than Pt/ACB. The instead higher activities given by Pt/NCB suggest that the NCB support has some sort of synergetic coupling effect in the ORR electrocatalysis. Since that the two catalysts were prepared in nearly the same procedures except that the two support materials were heat-treated under different gas environments, which renders that the NCB was nitrogen doped while the ACB was not, the synergetic effect should be a result of the nitrogen-doping.

As seen in Fig. 4b, the Pt/NCB exhibits more negative onset potential for Pt oxidation (~0.6 V) than the Pt/ACB (~0.7 V), which is in consistency with the general belief that smaller Pt particles bind the oxygenated species more strongly [33–35]. On the cathodic branch of the CVs, however, the peak potential for the reduction of the oxygenated adsorbates on Pt/NCB (~0.71 V) is slightly more positive than that of the Pt/ACB (~0.69 V), which

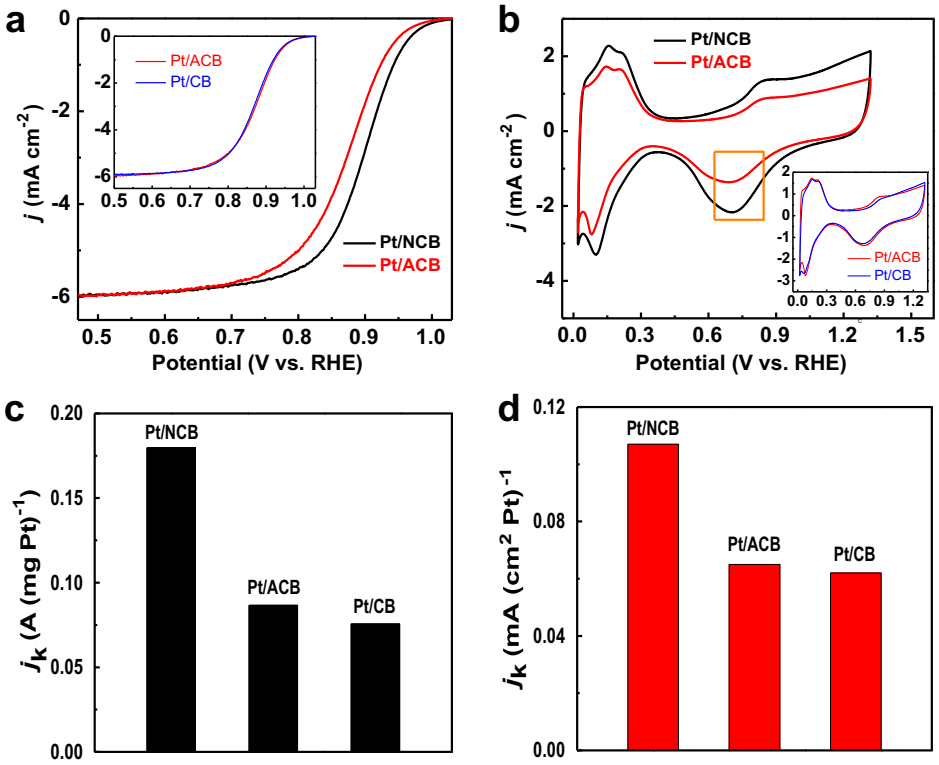

Fig. 4. Electrocatalytic properties of the prepared catalysts: (a) ORR polarization curves measured in O_2-saturated 0.1 M $HClO_4$ at a scan rate of 5 mv s^{-1} and electrode rotation rate of 1600 rmp; (b) CV curves measured in Ar-saturated 0.1 M $HClO_4$ at a scan rate of 50 mv s^{-1}; (c) mass and (d) area specific activities at 0.9 V versus RHE.

seems suggesting that the removal of the oxygenated species on Pt/NCB is easier, contradictory to the implication from the more negative onset potential for Pt oxidation that the smaller Pt particles on the NCB bind oxygenated species more strongly. Generally, one would expect a negative shift in peak potential for the reduction of the oxygenated species on smaller Pt nanoparticles [33–35]. Recently, Mayrhofer et al. [34] studied the particle size effect of the ORR on Pt nanoparticles in perchloric acid electrolyte. They showed that desorption of the oxygenated species was more difficulty and the area specific activity for the ORR was lower on smaller Pt particles. Sun et al. [35] found the similar trend when investigating the particle size effect of Pt in 0.5 M H_2SO_4 solution. The present results that the smaller Pt nanoparticles in the Pt/NCB exhibits a more negative onset potential for the Pt oxidation but more positive peak potential for the reduction of the oxygenated species (Fig. 4b) seems to suggest that the NCB support facilitate the desorption of the oxygenated species from Pt. This may be explained in terms of the spillover effect that the oxygenated species produced on Pt transport to the nearby C–N active center on NCB, which would result in lowered coverage of the oxygenated species on Pt. In general, the redox peaks associated with the formation and reduction of the oxygenated species are more reversible at lower coverage [36].

The increased area specific ORR activity on the Pt/NCB catalyst may be due to the above mentioned spillover effect, which is schematically illustrated in Fig. 5. Firstly, the oxygen molecules adsorbed on the surface of Pt nanoparticles can be dissociated to oxygen atoms (O). In addition to form H_2O through a further reaction on Pt, some of the adsorbed oxygen atoms may transport to the nearby C–N active center and are then further reduced to H_2O. The involvement of the C–N active sites on the NCB thus increases the overall ORR rate, therefore the apparent area specific activity of the supported Pt.

A question may be asked why the spillover of oxygenated species more easily occurs in the Pt/NCB catalyst. Recent studies have shown that N-doping can increase the oxophilicity of the carbon materials, making the N-doped carbons themselves can be ORR active [22]. However, N-doped carbons mainly exhibited superior ORR activities in alkaline [23,24], and remain poorly active in acidic media [24,25]. In alkaline media, the ORR takes place at considerably negative potentials, at which some extent of outer-sphere electron transfer between electrode and the physically adsorbed oxygen molecule may become possible [37]. That's might be the reason why the ORR can proceed in relatively less catalytic materials such as NCB. In acidic media, the chemical adsorption and/or dissociation of O_2 are necessary for the ORR to take place, while the N-doped carbons might not be oxophilic enough to initiate these steps. When N-doped carbons are used as support for Pt that are ORR active, however, the increased oxophilicity of N-doping carbons may facilitate the spillover of oxygenated intermediates produced on Pt nanoparticles to their surface. The oxygen spillover have been also found on the catalyst of Pt nanoparticles supported on TiO_2 [20] and $Y(OH)_3$ [21].

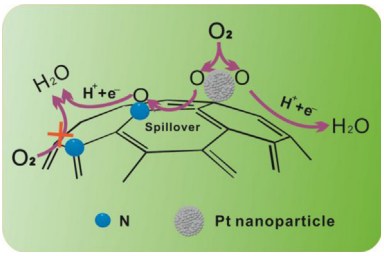

Fig. 5. Proposed mechanism for the improved ORR activity due to the oxygen spillover occurred on the catalyst of Pt nanoparticles supported on N-doped carbon support.

4. Conclusions

In summary, the electrochemical properties of Pt nanoparticles supported on carbon blacks heat-treated under argon and NH_3 were compared. The cyclic voltammetric responses of the two types of carbon-supported Pt nanoparticles suggests that spillover of the oxygenated intermediates produced on Pt to the active sites on NCB may take place, which, in one hand can increases the number of free sites on the surface of Pt nanoparticles for oxygen adsorption and dissociation, and in the other hand makes the surface sites on the N-doped carbon to participate in the ORR more efficiently.

Acknowledgements

This work was supported by the Ministry of Science and Technology (Grant Nos. 2012CB932800 and 2012AA110601), National Natural Science Foundation of China (Grant No. 21073137) and the Large-scale Instrument and Equipment Sharing Foundation of Wuhan University.

References

[1] M. Winter, R.J. Brodd, Chem. Rev. 104 (2004) 4245–4270.
[2] K. Sopian, W.R.W. Daud, Renew. Energy 31 (2006) 719–727.
[3] H.A. Gasteiger, N.M. Markoví, Science 324 (2009) 48–49.
[4] K.M. Metz, D. Goel, R.J. Hamers, J. Phys. Chem. C 111 (2007) 7260–7265.
[5] J. Zhang, K. Sasaki, E. Sutter, R.R. Adzic, Science 315 (2007) 220–222.
[6] J.F. Wu, X.Z. Yuan, J.J. Martin, H.J. Wang, J.J. Zhang, J. Shen, S.H. Wu, W. Merida, J. Power Sources 184 (2008) 104–119.
[7] M. Kim, S. Hwang, J.-S. Yu, J. Mater. Chem. 17 (2007) 1656–1659.
[8] R. Wang, X. Li, H. Li, Q. Wang, H. Wang, W. Wang, J. Kang, Y. Chang, Z. Lei, Int. J. Hydrogen Energy 36 (2011) 5775–5781.
[9] B. Choi, H. Yoon, I.-S. Park, J. Jang, Y.-E. Sung, Carbon 45 (2007) 2496–2501.
[10] Y.L. Hsin, K.C. Hwang, C.T. Yeh, J. Am. Chem. Soc. 129 (2007) 9999–10010.
[11] Y. Motoyama, Y. Lee, K. Tsuji, S.-H. Yoon, I. Mochida, H. Nagashim, ChemCatChem 3 (2011) 1578–1581.
[12] G. Vijayaraghavan, K.J. Stevenson, Langmuir 23 (2007) 5279–5282.
[13] M.S. Saha, R. Li, X. Sun, S. Ye, Electrochem. Commun. 11 (2009) 438–441.
[14] R.I. Jafri, N. Rajalakshmi, S. Ramaprabhu, J. Mater. Chem. 20 (2010) 7114–7117.
[15] G. Wu, D. Li, C. Dai, D. Wang, N. Li, Langmuir 24 (2008) 3566–3575.
[16] Y. Zhou, K. Neyerlin, T.S. Olson, S. Pylypenko, J. Bult, H.N. Dinh, T. Gennett, Z. Shao, R. O'Hayre, Energy Environ. Sci. 3 (2010) 1437–1446.
[17] Y. Shao, J. Sui, G. Yin, Y. Gao, Appl. Catal. B: Environ. 79 (2008) 89–99.
[18] B. Zheng, W.T. Zheng, K. Zhang, Q.B. Wen, J.Q. Zhu, S.H. Meng, X.D. He, J.C. Han, Carbon 44 (2006) 962–968.
[19] W.C. Conner, J.L. Falconer, Chem. Rev. 95 (1995) 759–788.
[20] H. Lin, J. Mol. Catal. A: Chem. 144 (1999) 189–197.
[21] K.G. Nishanth, P. Sridhar, S. Pitchumani, Electrochem. Commun. 13 (2011) 1465–1468.
[22] K. Gong, F. Du, Z. Xia, M. Durstock, L. Dai, Science 323 (2009) 760–764.
[23] Y. Zheng, Y. Jiao, M. Jaroniec, Y. Jin, S.Z. Qiao, Small 8 (2012) 3550–3566.
[24] D.S. Yu, E. Nagelli, F. Du, L.M. Dai, J. Phys. Chem. Lett. 1 (2010) 2165–2173.
[25] F. Charreteur, F. Jaouen, S. Ruggeri, J.-P. Dodelet, Electrochim. Acta 53 (2008) 2925–2938.
[26] Y. Dai, L. Ou, W. Liang, F. Yang, Y. Liu, S. Chen, J. Phys. Chem. C 115 (2011) 2162–2168.
[27] L. Qu, Y. Liu, J.-B. Baek, L. Dai, ACS Nano 4 (2010) 1321–1326.
[28] E. Yeager, J. Mol. Catal. 38 (1986) 5–25.
[29] K. Wiesener, Electrochim. Acta 31 (1986) 1073–1078.
[30] P.H. Matter, L. Zhang, U.S. Ozkan, J. Catal. 239 (2006) 83–96.
[31] B. Lim, M.J. Jiang, P.H.C. Camargo, E.C. Cho, J. Tao, X.M. Lu, Y.M. Zhu, Y.N. Xia, Science 324 (2009) 1302–1305.
[32] K. Kinoshita, J. Electrochem. Soc. 137 (1990) 845–848.
[33] H.A. Gasteiger, S.S. Kocha, B. Sompalli, F.T. Wagner, Appl. Catal. B: Environ. 56 (2005) 9–35.
[34] K.J.J. Mayrhofer, B.B. Blizanac, M. Arenz, V.R. Stamenkovic, P.N. Ross, N.M. Markovic, J. Phys. Chem. B 109 (2005) 14433–14440.
[35] Y. Sun, Y. Dai, Y.W. Liu, S.L. Chen, Phys. Chem. Chem. Phys. 14 (2012) 2278–2285.
[36] B.E. Conway, S. Gottesfeld, J. Chem. Soc. Faraday Trans. 69 (1973) 1090–1107.
[37] N. Ramaswamy, S. Mukerjee, Adv. Phys. Chem. 2012 (2012) 1–7.